THE JOURNAL OF PHYSICAL CHEMISTRY B

Article

Cite This: J. Phys. Chem. B 2018, 122, 4653−4661

pubs.acs.org/JPCB

Theoretical Investigations of the Role of Mutations in Dynamics of Kinesin Motor Proteins

Mikita Misiura,[†,‡] Qian Wang,[‡] Margaret S. Cheung,[‡,§] and Anatoly B. Kolomeisky*[,†,‡]

[†]Department of Chemistry and [‡]Center for Theoretical Biological Physics, Rice University, Houston, Texas 77005, United States

[§]Department of Physics, University of Houston, Houston, Texas 77204, United States

ABSTRACT: Motor proteins are active enzymatic molecules that are critically important for a variety of biological phenomena. It is known that some neurodegenerative diseases are caused by specific mutations in motor proteins that lead to their malfunctioning. Hereditary spastic paraplegia is one of such diseases, and it is associated with the mutations in the neuronal conventional kinesin gene, producing the decreased speed and processivity of this motor protein. Despite the importance of this problem, there is no clear understanding on the role of mutations in modifying dynamic properties of motor proteins. In this work, we investigate theoretically the molecular basis for negative effects of two specific mutations, N256S and R280S, on the dynamics of kinesin motor proteins. We hypothesize that these mutations might accelerate the adenosine triphosphate (ATP) release by increasing the probability of open conformations for the ATP-binding pocket. Our approach is based on the use of coarse-grained structure-based molecular dynamics simulations to analyze the conformational changes and chemical transitions in the kinesin molecule, which is also supplemented by investigation of a mesoscopic discrete-state stochastic model. Computer simulations suggest that mutations N256S and R280S can decrease the free energy difference between open and closed biochemical states, making the open conformation more stable and the ATP release faster, which is in agreement with our hypothesis. Furthermore, we show that in the case of N256S mutation, this effect is caused by disruption of interactions between α helix and switch I and loop L11 structural elements. Our computational results are qualitatively supported by the explicit analysis of the discrete-state stochastic model.

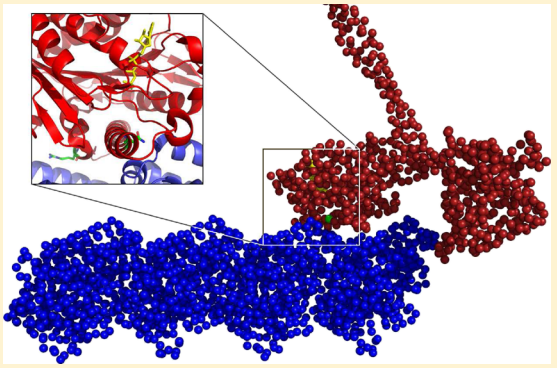

INTRODUCTION

Motor proteins, also known as biological molecular motors, are important players in multiple cellular processes such as intracellular transport, cell motility, muscle functioning, neuron dynamics, cell division, and transfer of genetic information.[1−4] Their specific biochemical function is to catalyze some biochemical processes, for example, the hydrolysis of adenosine triphosphate (ATP) or synthesis of nucleic acids and proteins.[3] A fraction of the energy released during these chemical reactions is converted then into a mechanical work needed for accomplishing their biological goals.[1−3] One of the main functions of motor proteins is to support the intracellular transport in which the biological molecular motors move cellular particles directionally along cytoskeleton filaments, such as microtubules (MTs) and actin filaments.[1−3]

There are many types of motor proteins in living organisms, but one of the most studied motors is a conventional kinesin, or kinesin-1, which is a member of a kinesin superfamily of motor proteins.[5] Kinesins play crucial roles in mitosis, neuron functioning, and many other aspects of the intracellular transport.[6−8] They fuel their motion by using the energy from ATP hydrolysis, but the molecular mechanisms of the energy conversion and consequent conformational changes remain not fully understood.[9,10] Kinesin is a dimer molecule that walks in a hand-over-hand manner along the MT, making up to a hundred of ∼8 nm steps in the plus direction of the filament before dissociating into the solution.[3,11,12] It consists of a motor domain and stalk and tail domains. The motor domain is responsible for ATP hydrolysis and for the attachment to MTs, whereas the tail domain connects kinesin to its cellular cargo through the linker proteins.[13,14] The motor domain is the most crucial part of kinesin because its conformational changes drive the directed motion along the filaments.[9,10] ATP binding stimulates neck linker docking with the motor domain, thus pushing the kinesin forward together with its cargo (toward the plus end of MT).

The importance of kinesins in cellular processes can be seen from the fact that malfunctionings of these molecular motors are frequently associated with a number of diseases. The majority of them are neurodegenerative diseases, and the reason for this is that neurons are highly asymmetric extended cells (some of them could be up to meters in length!), which depend much strongly on efficient transportation of cellular components than on any other typical cells in the living

Received: January 24, 2018
Revised: April 7, 2018
Published: April 9, 2018

DOI: 10.1021/acs.jpcb.8b00830
J. Phys. Chem. B 2018, 122, 4653−4661

systems.[15−17] One of these neurodegenerative diseases, called hereditary spastic paraplegia (HSP), is known to be associated with mutations in the part of the genome that contains a neuron-specific conventional kinesin's gene KIF5A.[18] Medical observations suggest that patients with the HSP exhibit weakness in the lower extremities and difficulties while walking.[19−21] However, the full understanding of the disease molecular origin is still lacking.

It is widely accepted that the malfunctioning of kinesin motor proteins is associated with mutations in them. At the same time, how specific mutations modify biochemical and biophysical properties of molecular motors remains not well-understood. In this paper, we investigate the effect of mutations on the dynamic properties of motor proteins by considering how two specific mutations, N256S and R280S, which are known to be related with the HSP disease,[20,22] change the dynamics of kinesin motor proteins. It is found by experimental observations that these specific mutations can lower the velocity, processivity, and MT-binding affinity of these biological motors.[22] We propose a hypothesis that these mutations can increase the ATP release rate in comparison with a wild-type (WT) protein. Because ATP in the mutated species does not have enough time to hydrolyze, it influences the enzymatic cycle, leading to the modified dynamic properties.[23] Extensive computer simulations using a structure-based molecular dynamics (MD) model are utilized to prove the validity of this hypothesis. Computational results are also supplemented with a simple discrete-state stochastic model to obtain a clear physical picture of the process. Our theoretical calculations provide a molecular picture on the effect of mutations on functioning of biological molecular motors.

METHODS

We employ a coarse-grained structure-based computational model, which was developed earlier in our group, to represent a kinesin-1 molecule associated with a segment of the MT filament (see Figure 1).[24] A 16 nm MT fragment (consisting of two tubulin subunits) with bound dimeric kinesin-1 is considered. The trailing head of the kinesin molecule is in the ATP-bound state, and it is attached to the MT. ATP is represented using positions of its heavy atoms,[25] while the rest of the model is a C_α model, that is, each aminoacid was represented as a single bead placed in the position of a C_α atom. The leading head is not attached to the MT, and it has no ATP molecule. The model was created using a SMOG server[26] with the following PDB structures: 3J8Y, 3J8X (motor heads in the nonnucleotide and ATP-bound states, MT, part of the neck linker), 3KIN (rest of the neck linker), and 1D7M (stalk domain).[32]

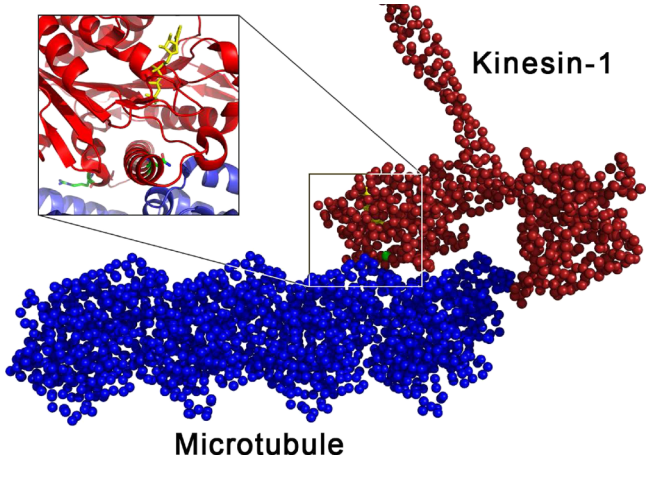

Figure 1. General view of the kinesin bound to the MT segment. Main picture shows a coarse-grained view, while the inset presents a full-atom model of the part of the system (using the PDB structure 3J8Y). The MT is shown in blue, the kinesin is shown in red, the ATP molecule is yellow, and N255 and R280 residues are green. The leading head is not attached to the MT. More details are given in the text.

The Hamiltonian of our system can be written as[27]

$$H = V_{\text{bond}} + V_{\text{DH}} + V_{\text{nb}} \tag{1}$$

In this equation, the first term represents the bonded interactions, which are given by a finite extensible nonlinear elastic potential

$$V_{\text{bond}} = \sum_{i,j} k \cdot R^2 \cdot \log\left(1 - \frac{(r_{ij} - r_{ij}^0)^2}{R^2}\right) \tag{2}$$

with spring constant $k = 3.75 \times 10^4$ kJ/mol·nm. The finite extensibility R is taken to be 0.2 nm, and r_{ij} is the distance between two adjacent beads i and j. The second term in eq 1 describes the Debye−Hückel screened electrostatic interactions between the charged beads within the kinesin molecule, as well as those between the kinesin and MT charged groups

$$V_{\text{DH}} = \sum_{i,j} \frac{q_i q_j}{4\pi\varepsilon\varepsilon_0 r_{ij}} \, \mathrm{e}^{-\kappa r_{ij}} \tag{3}$$

where the Debye length κ^{-1} is set to be 1 nm (corresponding to the ionic strength of 0.1 M, which is close to physiological conditions). The third term in eq 1 represents the nonbonded interactions. In our model, nonbonded interactions are given by Gaussian potentials instead of a standard Lennard-Jones potential. Gaussian potentials provide more control over the form of interactions. For example, they can be used to create two minima instead of one (dual-basin models) and to control the repulsion component independently from the attraction component. Both of these features are employed in this work. The ATP-bound trailing head in our model is represented via a dual-basin model, while the leading head without a nucleotide is analyzed via a single-basin model. For the single-basin model of the leading head of kinesin, we have

$$V_{\text{nb}} = \sum_{\text{native}} G(\varepsilon) + \sum_{\text{non-native}} \varepsilon_{\text{rep}} \left(\frac{\sigma_{\text{rep}}}{r_{ij}}\right)^{12} \tag{4}$$

where $G(\epsilon)$ is the Gaussian-like potential between particles i and j of the form

$$G(\varepsilon) = \varepsilon\left[\left(1 - \exp\left[-\frac{(r_{ij} - r_{ij}^0)^2}{2\sigma^2}\right]\right)\left(1 + \frac{1}{\varepsilon}\left(\frac{\sigma_{\text{rep}}}{r_{ij}}\right)^{12}\right) - 1\right] \tag{5}$$

In eq 4, the first summation is over all native contacts within the kinesin molecule and it has both attraction and repulsion components, while the second summation is over the nonnative contacts within the kinesin molecule and it has only the repulsion component.

DOI: 10.1021/acs.jpcb.8b00830
J. Phys. Chem. B 2018, 122, 4653−4661

For the dual-basin model of the trailing head of kinesin, we use

$$V_{nb} = \sum_{3J8X} G(\varepsilon_1) + \sum_{3J8Y} G(\varepsilon_2) + \sum_{native} G'(\varepsilon) + \sum_{ATP} G(\varepsilon_{ATP}) + \sum_{non\text{-}native} \varepsilon_{rep}\left(\frac{\sigma_{rep}}{r_{ij}}\right)^{12} \quad (6)$$

where $G'(\epsilon)$ is equal to

$$G'(\varepsilon) = \varepsilon\left[\left(1 - \exp\left(-\frac{(r_{ij} - r_{ij}^0)^2}{2\sigma^2}\right)\right)\left(1 - \exp\left(-\frac{(r_{ij} - r_{ij}^{0'})^2}{2\sigma^2}\right)\right)\left(1 - \frac{1}{\varepsilon}\left(\frac{\sigma_{rep}}{r_{ij}}\right)^{12}\right) - 1\right] \quad (7)$$

In eq 6, the first term is for all the contacts that exist only in 3J8X, the second term takes into account the contacts only in 3J8Y, while the third term is for those contacts that exist in both 3J8X and 3J8Y. The first three terms also include interactions between the trailing head and the MT, extracted from structures 3J8X, 3J8Y, or both. The fourth term corresponds to the interactions between the kinesin molecule and ATP, which are single-basin, unlike the rest of interactions in the trailing head. The last term describes repulsion between all noninteracting beads. The list of native contacts was determined using a Shadow Map algorithm.[28] The standard deviation of a Gaussian function σ is equal to 0.03 nm; the van der Waals radius of a bead, σ_{rep}, is assumed to be 0.38 nm; the solvent-mediated interaction ϵ is set to 1.88 kJ/mol; ϵ_1 is taken to be 1.88 kJ/mol; ϵ_2 is assumed to be 1.01 kJ/mol; and ϵ_{ATP} is equal to 0.23 kJ/mol. The coefficient to scale the repulsions between the nonnative contacts, ϵ_{rep}, is also set to 1.88 kJ/mol as well.

The model described above corresponds to the WT kinesins, and more details can be found in ref 24. To obtain the corresponding description for the mutated kinesin-1 molecule, we modified the nonbonded interactions of the mutated residue to make them twice as strong or to remove them completely. This procedure can be explained using the following arguments. The mutated residue most probably will either form stronger interactions with surrounding aminoacids or it will not form them at all. Doubling of the strength of interactions involved setting ϵ to 3.75 kJ/mol, and the case of no interactions leads to $\epsilon = 0$. This way we can modify equally the interactions existing in both the nonnucleotide and ATP-bound states. Thus, five models of different kinesin molecules were created: the WT with the intact interactions (WT model), two N256S mutant models with all interactions of N256 removed (256 None) or with the doubled strength (256 Double), and two R280S mutant models with all interactions of R280 removed (280 None) or with the doubled strength (280 Double). This procedure allows us to test consistently the effect of these specific mutations.

MD simulations were performed using GROMACS 4.5.4 software package.[29,30] SMOG[26] with the Shadow contact map method was utilized to generate C_α models. For each version of the kinesin molecule, there were 24 to 30 MD trajectories collected with 50 000 000 integration steps in each. Coordinates of the system were written every 1000 steps, totaling in 50 000 samples per trajectory. Only positions of kinesin's atoms were integrated, while the MT atoms were frozen. We employed the Langevin equations of motion for the coarse-grained molecular simulations. Langevin equations of motion were integrated in the low friction limit with a damping coefficient of $1\tau_L^{-1}$. The integration time step is $10^{-3}\tau_L$, where $\tau_L = \sqrt{(m\sigma^2/\varepsilon)}$, m is the mass of a bead, ϵ is the solvent-mediated interaction, and σ is the van der Waals radius of a C_α bead. The constant volume and temperature of 300 K were maintained during these simulations (NVT ensemble). No periodic boundary conditions were utilized.

The gyration radius of the ATP-binding pocket was used as a reaction coordinate to measure the free energy difference between open and closed conformations for different kinesin species. Detailed calculations of the gyration radius are presented in ref 24. From each trajectory, a distribution of gyration radii was obtained and after a logarithmic transformation differences in the heights of peaks of open and closed conformations were measured. Errors were estimated by applying a bootstrap technique where the measured free energy differences from each trajectory were used as independent data points. Contact maps were calculated for each trajectory and then averaged. The shadow contact map method[26] was applied to generate a list of contacts, and the contact was considered to be present if the distance between two aminoacids was within 10% margin as compared to an equilibrium value; that is, if the equilibrium distance is r_0, then the contact was considered to exist in these snapshots of MD simulation where the distance was between $0.9r_0$ and $1.1r_0$. In our model, these cutoffs ranged from 3.4 to 21.3 Å.

RESULTS AND DISCUSSION

Mutations N256S and R280S Can Increase the ATP Release Rate of Kinesin. Experimental data[22,36] show that the mutations N256S and R280S reduce the speed of kinesin-1 by factors of 4.3 and 1.2, respectively. To explain these observations at the molecular level, we propose that these mutations increase the probability of the open conformations for the ATP-binding pocket. Such conformational changes can accelerate the release rates of the nucleotides (ATP and ADP). It is expected that this will lower the velocity of the mutated kinesin-1 molecule. If the system does not have enough time to hydrolyze ATP, the enzymatic cycle will not be completed, and the motor protein will not advance. Many conformational transitions must take place before the successful hydrolysis event, and this should slow down the motor protein's speed.

To test this hypothesis, we ran coarse-grained structure-based MD simulations for each molecular model of the kinesin-1 as described in the "Methods" section. To measure if the ATP-binding site is open or closed, we used the gyration radius calculated using the aminoacids forming this binding site. The idea here is that a more open conformation has a larger radius of gyration. Mutations in the region close to the ATP-binding pocket have the potential to modify this free energy difference and hence to change the probability of the open state of the ATP-binding pocket. Because ATP prefers to unbind from the open conformation, this will obviously affect kinesin's ATP-binding affinity, eventually modifying its dynamic properties.

Computed free energy differences for all five models of kinesin-1 are presented in Table 1 and Figure 2. One can see that for all different kinesin species, the closed conformations are more preferred because they have lower free energies.

DOI: 10.1021/acs.jpcb.8b00830
J. Phys. Chem. B 2018, 122, 4653−4661

Table 1. Computed Free Energy Differences between Open and Closed Conformations of the ATP-Binding Pocket in Kinesin-1 ($\Delta E = E_{open} - E_{closed}$) and the Average Fraction of the Native Contacts between ATP and Kinesin-1 for All Five Kinesin-1 Models

kinesin	ΔE, k_BT	$\langle Q_{ATP} \rangle$
WT	1.91 ± 0.05	0.784 ± 0.003
256 None	1.39 ± 0.07	0.739 ± 0.003
256 Double	1.92 ± 0.05	0.794 ± 0.002
280 None	1.69 ± 0.06	0.734 ± 0.003
280 Double	1.92 ± 0.06	0.78 ± 0.01

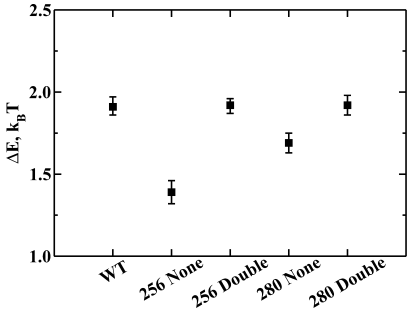

Figure 2. Free energy differences between open and closed conformations of the ATP-binding pocket ($\Delta E = E_{open} - E_{closed}$) for various kinesin-1 models.

However, the free energy differences vary as a function of the position of the mutation and the strength of the additional interaction due to the mutation. For the N256S mutation without interactions, the free energy difference decreases by about 0.5 k_BT, making the open configuration relatively more probable than in the WT case. Figure 3 shows probability

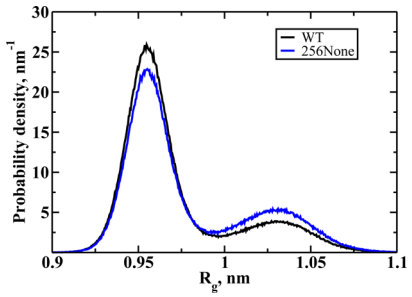

Figure 3. Probability density distributions of the gyration radius of the ATP-binding pocket for WT and 256 None models. Left maximum corresponds to closed conformation of the ATP-binding pocket, right maximum—to open conformation.

density distributions for WT and 256 None kinesin models. One can clearly see that probability of open conformation (maximum with higher R_g) is more probable in the 256 None model. A similar but weaker effect is observed for the R280S mutation without interactions: the free energy difference decrease here by 0.2 k_BT. However, both mutations with double interactions produce the same free energy difference as in the WT case. It seems that for both cases, stronger interactions might effectively compensate for the presence of mutations.

Our results suggest that the mutations lead to the increased probability for open conformations of the ATP-binding pocket. To understand how such a behavior influences the interactions between ATP and kinesin, we measured the fraction of the native contact formations between the ATP and kinesin molecules, Q_{ATP}. The physical meaning of this quantity is that the lower Q_{ATP} indicates a weaker binding, whereas the larger Q_{ATP} describes a stronger association. It is found that for the WT kinesin, Q_{ATP} is 0.78. This value drops to 0.74 and 0.73 for 256 None and 280 None mutations, respectively. Therefore, the interactions between ATP and kinesin are indeed weakened because of the increased fraction of the open conformations in the kinesin, which is consistent with our hypothesis.

It is well-known that the mechanochemical cycle of kinesin consists of the ATP binding to the kinesin molecule, and the hydrolysis is taking place while the ATP-binding site is in the closed conformation. After that, the hydrolysis products are released when the ATP-binding pocket opens up.[1−3] Then, any process that disrupts this sequence of events will clearly influence the enzymatic efficiency of the motor protein, which leads to the modified dynamic properties. Making closed ATP-binding pocket configuration less probable because of the mutation will decrease the time for ATP in the catalytically preferable position, and the ATP molecule might leave the pocket before the hydrolysis can start. This interrupts the mechanochemical cycle, and more binding events will be needed before the enzymatic cycle might successfully proceed forward. We think that this might be a leading factor in the molecular mechanism of how the mutations N256S and R280S affect the dynamics of conventional kinesins. At the same time, it is possible that other mechanisms might also contribute for N256S and R280S. Furthermore, completely different mechanisms might be followed for other mutations.

Overall, the results of the extensive coarse-grained MD simulations are in agreement with our hypothesis that the mutations N256S and R280S lower kinesin's speed by increasing the ATP release rate from the catalytic site. This process decreases the residence time for ATP inside the enzymatic pocket, lowering the probability of hydrolysis and thus preventing the molecular motor from fast forward motion. Evolutionary analysis (data not shown) shows that both N256 and R280 are highly conservative, which confirms the important role of these residues inside kinesin's head.[31]

One could also suggest that the mutation might influence MT-biding affinity of the motor protein molecule because the location of these mutations is close to MT. To test this idea, we analyzed contact maps between MT and kinesin (results are not shown) and found that they are not altered (the maximum difference of the probability of contacts between the WT and 256 None models was found to be less than 0.2%, which is approximately 100 times smaller than the maximum difference for the data we presented in the manuscript). For this reason, the MT binding affinity is probably less affected by the mutations compared to the mechanism we proposed in this paper.

Mutation N256S Disrupts Interactions between α4 Helix and Loop L11. Because our data show that the deletion of the nonbonded interactions in N256S and R280S species produces the decrease in free energy difference between the open and closed conformations of the ATP-binding pocket, it is interesting to determine what contacts, among those that were deleted, contribute the most to this change. For this purpose, we utilized a method of contact maps, as presented in Figure 4. In the contact map, both axes show the amino acid numbers in protein's sequence, and the color on the intersection represents a probability of a contact being present between two specific

DOI: 10.1021/acs.jpcb.8b00830
J. Phys. Chem. B 2018, 122, 4653−4661

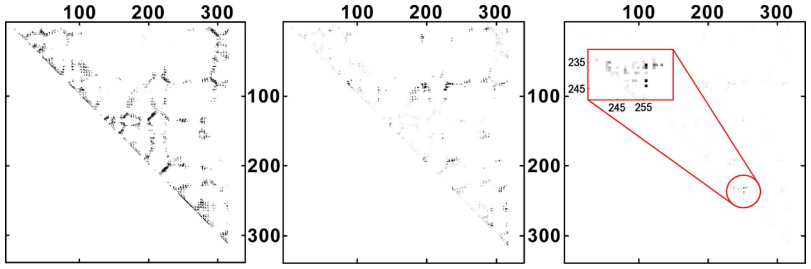

Figure 4. Left: Contact maps of WT kinesin-1 in our structure-based model. Symbols show probability of a contact between aminoacids during MD runs. Darker color means higher probability. Center: "Transition map": difference between contact maps for open and closed conformations of the ATP-binding pocket. Darker symbols show parts of the kinesin that change their contacts more during the open−closed transition. Right: Difference between "transition maps" between the WT and 256 None models. Inset shows in more detail the region with the maximal differences.

aminoacids at any moment during the MD simulation. These probabilities will be different for open and closed conformations of the ATP-binding pocket, underlining the differences between these conformations. Thus, the difference between the contact maps for the open and closed conformations of kinesin-1 ("transition map") can characterize these open−closed transitions. It is important to note that this map can also specify what specific residues are responsible for these transitions. The difference between the obtained "transition maps" for the WT and the mutated kinesin-1 models can show us how the open−closed transition are modified when the mutations are introduced.

An illustration of the analysis of contact maps is presented in Figure 5. It shows that in the case of the N256S mutant (model

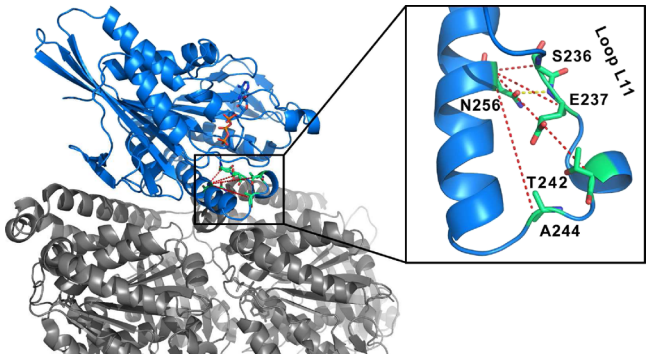

Figure 5. Structural view of the relevant contacts that are being modified in mutations. Contacts between N256 and loop 11 are disrupted as a result of the N256S mutation. Disrupted contacts are shown in red, and the respective aminoacids are shown in green. Note that only one of these contacts is real (hydrogen bond between N256 and E237 shown in yellow), and the rest of them exists only in the model. The MT is shown in gray, and kinesin's head is presented in blue (image generated from the PDB entry 3J8Y).

with no interactions of N256), probabilities of four contacts between N256 and a region called loop L11 are being significantly altered (Figure 5). In a full-atom structure of WT kinesin-1 (PDB: 3J8Y), the amide group of N256 forms hydrogen bonds with backbone atoms of E237, which in its turn forms a salt bridge with R204. This chain of contacts is likely to be disrupted or significantly altered upon the mutation. R204 is a residue on a so called Switch I loop, which together with loop L11 plays an important role in the ATP-binding process. These changes occur very close to the ATP-binding site and could easily affect the stability of corresponding conformations.

Similar analysis for the R280S mutation did not reveal any significant changes: all the contacts seem to change more or less equally. This is also consistent with the fact that the free energy difference for this mutant is less than that for the 256 mutation. This observation suggests that a computational model with more atomic details is probably needed to explain the effect of the R280S mutation.

Discrete-State Stochastic Model. To understand better the molecular effect of mutations on dynamics of motor proteins, we developed a simplified discrete-state stochastic model. Here, we extended the earlier theoretical approach,[33−35] which was already successfully utilized to describe and analyze single-molecule experimental measurements on kinesin-1. In this model, each kinesin's 8 nm step along the MT is viewed as a sequence of N biochemical states. The simplest model with $N = 2$ states is considered here, but we also take into account the open and closed conformations of the ATP-binding pocket, as illustrated in Figure 6.

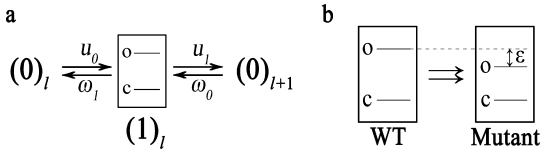

Figure 6. Schematic view of the discrete-state stochastic model to describe the effect of mutations in kinesins. (a) Two-state model of the kinesin's mechanochemical cycle. State (1) is considered to be a complex state: it has two distinct conformations with different energies—a closed state (labeled as c) and an open state (labeled as o). (b) Illustration of the effect of mutation. Mutation in kinesin changes the relative energies of the open and closed conformations of kinesin.

In the scheme presented in Figure 6a, the states $(0)_l$ and $(0)_{l+1}$ represent the kinesin molecule bound to the MT but without the ATP molecule, before and after the step of 8 nm, respectively. The state $(1)_l$ corresponds to the kinesin molecule bound to the MT after ATP binding. The forward transition rates from the states 0 and 1 are equal to u_0 and u_1, respectively, while the corresponding backward rates are w_1 and w_0: see Figure 6. Clearly, it is a strong approximation to view the processes after ATP binding as a single biochemical transition. Several processes are taking place at this stage, including multiple openings and closings of the ATP pocket, the hydrolysis of the ATP molecule, and the release of the hydrolysis products. Here, we assume that the equilibrium between the closed and open conformations of the ATP pocket is a dominating process and it determines the overall free

DOI: 10.1021/acs.jpcb.8b00830
J. Phys. Chem. B 2018, 122, 4653−4661

energy of the combined state 1. Then, the mutations that shift this equilibrium will change the transition rates into this state and out of this state, and the dynamic properties of the motor protein will be modified. This is the main idea of our simplified theoretical model.[36]

To make our arguments quantitative, we introduce a parameter ε that describes the difference in the free energies between the open and closed conformations in the mutated protein in comparison with the WT species: see Figure 6. Then, it can be argued that state 1 for the mutated kinesin has a free energy equal to ε. We also assume that lowering the free energy difference between the open and closed conformations decreases the free energy of state 1, while larger free energy differences lead to the lower free energy of state 1. In our model, the WT kinesin corresponds to $\varepsilon = 0\ k_BT$, while for the mutants N256S and R280S, the free energies of state 1 are equal to $\varepsilon = -0.52\ k_BT$ and $\varepsilon = 0.22\ k_BT$, respectively (see Table 1). This change should also alter the transitions rates for the mutants in the following way: u_1 and w_1 will decrease, while u_0 and w_0 will increase. More specifically, for the ratios of the transition rates we can write, using the detailed balance-like arguments

$$\frac{u_0}{w_1} = \frac{u_0^{(0)}}{w_1^{(0)}} \exp(-\beta\varepsilon) \tag{8}$$

$$\frac{u_1}{w_0} = \frac{u_1^{(0)}}{w_0^{(0)}} \exp(\beta\varepsilon) \tag{9}$$

where $\beta = 1/k_BT$ and $u_0^{(0)}$, $u_1^{(0)}$, $w_0^{(0)}$, and $w_1^{(0)}$ are transition rates for the WT kinesin molecule. The physical meaning of these expressions is that it is faster to enter state 1 and it is slower to leave state 1 in the mutated molecules in comparison with the WT kinesins.

To calculate dynamic properties of motor proteins, we need to have explicit expressions for the transitions rates. One can then introduce splitting parameters θ_1 and θ_2 which specify how the free energy shift ϵ affects the entrance and exit rates to state 1

$$u_0 = u_0^{(0)} \exp(-\beta\theta_1\varepsilon) \tag{10}$$

$$u_1 = u_1^{(0)} \exp(\beta\theta_2\varepsilon) \tag{11}$$

$$w_0 = w_0^{(0)} \exp(-\beta(1-\theta_2)\varepsilon) \tag{12}$$

$$w_1 = w_1^{(0)} \exp(\beta(1-\theta_1)\varepsilon) \tag{13}$$

One should also take into account the dependence of the transition rates on external forces, as was investigated in detail earlier.[33] This leads to

$$u_0^{(0)}(F) = u_0^{(0)}(F=0) \exp(-\theta_0^{+}Fd/k_BT) \tag{14}$$

$$u_1^{(0)}(F) = u_1^{(0)}(F=0) \exp(-\theta_1^{+}Fd/k_BT) \tag{15}$$

$$w_0^{(0)}(F) = w_0^{(0)}(F=0) \exp(\theta_0^{-}Fd/k_BT) \tag{16}$$

$$w_1^{(0)}(F) = w_1^{(0)}(F=0) \exp(\theta_1^{-}Fd/k_BT) \tag{17}$$

We also assume that the rate $u_0^{(0)}$ is proportional to the concentration of ATP, so that $u_0^{(0)} = k_0^{(0)}\cdot[\mathrm{ATP}]$, which reflects the fact that the transition from state 0 to state 1, describes the ATP binding to the motor protein molecule.

The load-dependent dynamics of kinesin motor proteins have been analyzed before, and it was found that the following parameters can describe single-molecule experimental data:[33] $\theta_0^{+} = 0.135$, $\theta_1^{+} = 0.035$, $\theta_0^{-} = 0.750$, $\theta_1^{-} = 0.080$, $k_0^{(0)} = 1.8\ \mu\mathrm{M}^{-1}\ \mathrm{s}^{-1}$, $w_1^{(0)} = 6.0\ \mathrm{s}^{-1}$, $u_1^{(0)} = 108\ \mathrm{s}^{-1}$, $w_0^{(0)} = 2.8 \times 10^{-4}\ \mathrm{s}^{-1}$, and $d = 8.2$ nm. We take these parameters as a description of the WT kinesins in our model, assuming the concentration of ATP molecules, [ATP] = 2 mM. However, for the mutants, we also need to determine the splitting coefficients θ_1 and θ_2. These parameters were fitted using experimental data,[22] and the results are presented in Figure 7. It is found that $\theta_1 = 0$ and $\theta_2 = 1$ describe the data in the best way (although note that there is a very limited amount of quantitative data available), which indicates that only the transitions rates associated with leaving state 1 are affected by these mutations (u_1 and w_1). This is consistent with our idea that mutations primarily influence unbinding of ATP or ADP molecules.

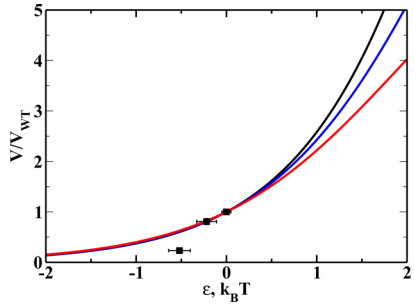

Figure 7. Normalized velocities of kinesin molecules as a function of the parameter ε. The WT kinesin corresponds to $\varepsilon = 0\ k_BT$. The lines represent theoretical predictions (black curve is for $F = 0$ pN, blue curve is for $F = 4$ pN, red curve is for $F = 7$ pN). Symbols are experimental data from ref 22. To the left on the graph, the probability of open conformation of the ATP-binding pocket increases, and to the right, it decreases.

Using the obtained parameters and expressions for the transitions rates, the velocity of various kinesin motor proteins can be calculated using the existing theoretical framework[33]

$$V = d\frac{(u_0u_1 - w_0w_1)}{u_0 + u_1 + w_0 + w_1} \tag{18}$$

where d is the motor protein step size. Figure 7 shows how the speeds of kinesins motor proteins are affected by the free energy shift ε. Mutations that correspond to the negative shifts (smaller difference between closed and open conformations), which also decrease the free energy of state 1, lower the speeds of molecular motors. This is the case for the mutations N256S and R280S, which is in agreement with experimental observations. Our model can also make several other predictions. First, we suggest that mutations that increase the energy shift between open and close conformations (positive ε) would lead to faster motion of the motor proteins in comparison with the WT species, and it will be force-dependent. Second, the mutations that lower the gap between the open and closed conformations (negative ε) would slow down the motor protein, but the velocities will be mostly insensitive to the external loads.

One can also see that our model, although describing the effect of mutations qualitatively, underestimates the effect of the N256S mutation. This can be explained because of a very simplified nature of the discrete-state model and the coarse-

DOI: 10.1021/acs.jpcb.8b00830
J. Phys. Chem. B 2018, 122, 4653−4661

grained nature of our MD simulations. However, some other additional features of this mutation might not be captured in our theory.

Using the same theoretical framework,[33] we can also estimate the effect of mutations on the processivity of kinesin motor proteins. The mean run length for each molecular motor can be calculated using the following formula

$$L = \frac{V}{P_0\delta_0 + P_1\delta_1} \tag{19}$$

where P_i is a stationary-state probability for the motor to be found in the state i (i = 1, 2), and δ_i is a detachment rate from state i, which has the following dependence on the external loads[33]

$$\delta_i(F) = \delta_i^{(0)} \exp(-\theta_i^{(\delta)} Fd/k_BT) \tag{20}$$

where $\delta_i^{(0)}$ is the detachment for F = 0 pN and $\theta_i^{(\delta)}$. Using the parameters obtained for the WT kinesins,[33] the results of our calculations for the processivity are presented in Figure 8. It is found that the mean run length will decrease for the negative ε and increase for the positive ε. Because the mutations N256S and R280S correspond to the negative free energy shifts, our theory predicts that the processivity for the mutants will be lower than for the WT kinesins. This result fully agrees with experimental observations.[22] It also suggests that the mechanism of the lowering of processivity can be explained by the increased time needed to complete the mechanochemical cycle of kinesin. Indeed, if we increase the probability of open conformation of the ATP-binding pocket, corresponding to a higher probability of the premature dissociation of ATP, this will increase the average time needed to hydrolyze the ATP molecule and to complete the mechanochemical cycle with advancing a distance of 8 nm. Then, for the same average times before the dissociation from the MT, the motor protein will make shorter runs, leading to the reduced processivity.

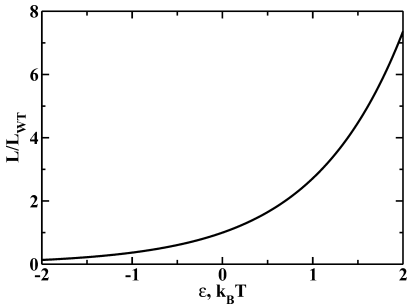

Figure 8. Normalized mean run lengths of the kinesin molecule as a function of the parameter ε (F = 0 pN). The WT kinesin corresponds to ε = 0 k_BT. To the left on the graph, the probability of open conformation of the ATP-binding pocket increases, and to the right, it decreases.

SUMMARY AND CONCLUSIONS

We present a comprehensive theoretical study on the effect of mutations on dynamic properties of processive motor proteins. Our approach combines extensive coarse-grained structure-based MD computer simulations with the explicit analysis of the mesoscopic discrete-state stochastic model. It is applied for the investigation of the role of specific mutations N256S and R280S, which are found to be associated with the HSP neurodegenerative disease. Our theoretical analysis has been driven by the proposed hypothesis that these mutations accelerate the premature release of ATP molecules after binding by increasing the probability of open conformations for the ATP-binding pocket. MD computer simulations indicate that the mutations N256S and R280S indeed can lead to the higher probability of the open state of the ATP-binding pocket, reducing the average number of contacts between ATP and the kinesin. It is found that this might be the result of decreasing the number of interatomic contacts or due to the changes in the interactions between the side chains of the mutated residues compared to the WT side chains. Furthermore, in the case of N256S mutation, specific structural observations support this argument. To make a connection between structural changes and dynamic properties of motor proteins more quantitative, the effect of mutations was also analyzed using the discrete-state stochastic model. It was shown that the mutations lead to changes in the free energy difference between open and closed conformations, which affects the transitions rates and eventually modifies the dynamic properties. Using the free energy shifts computed in our MD simulations, velocities and mean run lengths of the motor proteins have been explicitly calculated. In agreement with experimental observations, it is found that mutations, which decrease the free energy difference between open and closed configurations, slow down molecular motors and decrease their processivity. It was argued that this is the consequence of effectively lowering the free energy of the combined biochemical state that describes the processes after ATP binding to the MT-bound kinesin molecule. Experimental data[37] show that the ATP release occurs on the same time scale as ATP hydrolysis: rate constants of these processes for WT kinesin are 71 and 100 s^{-1}, respectively, and one expects that the ATP release rate is likely to be even higher for mutated kinesins. These data suggest that any changes in the ATP release are very likely to affect the overall rate of kinesin's cycle, which is in line with our hypothesis.

It should be noted that our simulations were done at the fixed ATP concentration. One could also argue that in the case of larger ATP concentrations, the effect of the energy shift between open and closed conformations would be less important. This is because any released ATP molecule will be very quickly substituted by another ATP molecule, reducing the lifetimes of the open conformations. In this case, other biochemical transitions will define the overall dynamics of the kinesin motor proteins.

Although our theoretical approach was able to explain the effect of specific mutations in the kinesin motor proteins, providing microscopic connections between the structural modifications and the changes in dynamic properties, there are several potential issues associated with the approximations utilized in our method. In MD computer simulations, the coarse-grained model considered every aminoacid as an effective particle, neglecting the chemical composition variations that might affect the interactions in the system. We also utilized an implicit solvent, the MT segment was considered to be frozen, and we employed Gaussian interactions instead of the widely utilized Lennard-Jones potentials. Other processes, such as changes in the MT binding affinity and the phosphate release, might also be affected by the mutations, but our method cannot capture these effects. In the discrete-state stochastic model, the complex biochemical description of the motor protein was reduced to a very crude two-state description. In addition, it was assumed that lowering

DOI: 10.1021/acs.jpcb.8b00830
J. Phys. Chem. B 2018, 122, 4653−4661

the free energy difference between open and closed conformations should lower the free energy of the system. More advanced theoretical methods are needed to test the validity of these approximations. However, despite these issues, our theoretical method provides a semiquantitative description of the effect of mutations in motor proteins with experimentally testable predictions, which can further advance our knowledge on the mechanisms of biological processes.

AUTHOR INFORMATION

Corresponding Author

*E-mail: tolya@rice.edu.

ORCID

Anatoly B. Kolomeisky: 0000-0001-5677-6690

Notes

The authors declare no competing financial interest.

ACKNOWLEDGMENTS

This work is supported by Center for Theoretical Biological Physics NSF grant PHY-1427654. A.B.K. also acknowledges the support from Welch Foundation (grant C-1559) and from the NSF (grant CHE-1664218). M.S.C. also acknowledges the support from the NSF (grant MCM-1412532).

REFERENCES

(1) Alberts, B. *Molecular Biology of the Cell*, 6th ed.; Garland Science: New York, 2014.

(2) Lodish, H. *Molecular Cell Biology*, 6th ed.; W. H. Freeman and Company: New York, 2007.

(3) Kolomeisky, A. B. *Motor Proteins and Molecular Motors*; CRC Press, 2015.

(4) Jolly, A. L.; Gelfand, V. I. Bidirectional Intracellular Transport: Utility and Mechanism. *Biochem. Soc. Trans.* **2011**, *39*, 1126−1130.

(5) Hirokawa, N. Kinesin and Dynein Superfamily Proteins and the Mechanism of Organelle Transport. *Science* **1998**, *279*, 519−526.

(6) Straube, A.; Hause, G.; Fink, G.; Steinberg, G. Conventional Kinesin Mediates Microtubule-Microtubule Interactions in Vivo. *Mol. Biol. Cell* **2006**, *17*, 907−916.

(7) Sheetz, M. P. What are the Functions of Kinesin? *BioEssays* **1987**, *7*, 165−168.

(8) Wordeman, L.; Mitchison, T. J. Identification and Partial Characterization of Mitotic Centromere-Associated Kinesin, a Kinesin-Related Protein That Associates with Centromeres During Mitosis. *J. Cell Biol.* **1995**, *128*, 95−104.

(9) Asenjo, A. B.; Weinberg, Y.; Sosa, H. Nucleotide Binding and Hydrolysis Induces a Disorder-Order Transition in the Kinesin Neck-Linker Region. *Nat. Struct. Mol. Biol.* **2006**, *13*, 648.

(10) Rice, S.; Lin, A. W.; Safer, D.; Hart, C. L. A Structural Change in the Kinesin Motor Protein That Drives Motility. *Nature* **1999**, *402*, 778.

(11) Yildiz, A.; Tomishige, M.; Vale, R. D.; Selvin, P. R. Kinesin Walks Hand-Over-Hand. *Science* **2004**, *303*, 676−678.

(12) Vale, R. D.; Milligan, R. A. The Way Things Move: Looking Under the Hood of Molecular Motor Proteins. *Science* **2000**, *288*, 88−95.

(13) Seiler, S.; Kirchner, J.; Horn, C.; Kallipolitou, A.; Woehlke, G.; Schliwa, M. Cargo Binding and Regulatory Sites in the Tail of Fungal Conventional Kinesin. *Nat. Cell Biol.* **2000**, *2*, 333.

(14) Horiuchi, D.; Collins, C. A.; Bhat, P.; Barkus, R. V.; DiAntonio, A.; Saxton, W. M. Control of a Kinesin-Cargo Linkage Mechanism by JNK Pathway Kinases. *Curr. Biol.* **2007**, *17*, 1313−1317.

(15) Hurd, D. D.; Saxton, W. M. Kinesin Mutations Cause Motor Neuron Disease Phenotypes by Disrupting Fast Axonal Transport in Drosophila. *Genetics* **1996**, *144*, 1075−1085.

(16) Goldstein, L. S. B. Kinesin Molecular Motors: Transport Pathways, Receptors, and Human Disease. *Proc. Natl. Acad. Sci. U.S.A.* **2001**, *98*, 6999−7003.

(17) Mandelkow, E.; Mandelkow, E.-M. Kinesin Motors and Disease. *Trends Cell Biol.* **2002**, *12*, 585−591.

(18) Wang, L.; Brown, A. A Hereditary Spastic Paraplegia Mutation in Kinesin-1A/KIF5A Disrupts Neurofilament Transport. *Mol. Neurodegener.* **2010**, *5*, 52.

(19) Lo Giudice, M.; Neri, M.; Falco, M.; Sturnio, M.; Calzolari, E.; Di Benedetto, D.; Fichera, M. A Missense Mutation in the Coiled-Coil Domain of the KIF5A Gene and Late-Onset Hereditary Spastic Paraplegia. *Arch. Neurol.* **2006**, *63*, 284−287.

(20) Reid, E.; Kloos, M.; Ashley-Koch, A.; Hughes, L.; Bevan, S.; Svenson, I. K.; Graham, F. L.; Gaskell, P. C.; Dearlove, A.; Pericak-Vance, M. A.; et al. A Kinesin Heavy Chain (KIF5A) Mutation in Hereditary Spastic Paraplegia (SPG10). *Am. J. Hum. Genet.* **2002**, *71*, 1189−1194.

(21) Depienne, C.; Stevanin, G.; Brice, A.; Durr, A. Hereditary Spastic Paraplegia: An Update. *Curr. Opin. Neurol.* **2007**, *20*, 674−680.

(22) Ebbing, B.; Mann, K.; Starosta, A.; Jaud, J.; Schöls, L.; Schüle, R.; Woehlke, G. Effect of Spastic Paraplegia Mutations in KIF5A Kinesin on Transport Activity. *Hum. Mol. Genet.* **2008**, *17*, 1245−1252.

(23) Zhang, Z.; Goldtzvik, Y.; Thirumalai, D. Parsing the roles of neck-linker docking and tethered head diffusion in the stepping dynamics of kinesin. *Proc. Natl. Acad. Sci. U.S.A.* **2017**, *114*, E9838−E9845.

(24) Wang, Q.; Diehl, M. R.; Jana, B.; Cheung, M. S.; Kolomeisky, A. B.; Onuchic, J. N. Molecular Origin of the Weak Susceptibility of Kinesin Velocity to Loads and Its Relation to the Collective Behavior of Kinesins. *Proc. Natl. Acad. Sci. U.S.A.* **2017**, *114*, E8611−E8617.

(25) Tehver, R.; Thirumalai, D. Rigor to Post-Rigor Transition in Myosin V: Link Between the Dynamics and the Supporting Architecture. *Structure* **2010**, *18*, 471−481.

(26) Noel, J. K.; Whitford, P. C.; Sanbonmatsu, K. Y.; Onuchic, J. N. SMOG@ctbp: Simplified Deployment of Structure-Based Models in GROMACS. *Nucleic Acids Res.* **2010**, *38*, W657−W661.

(27) Zhang, Z.; Thirumalai, D. Dissecting the Kinematics of the Kinesin Step. *Structure* **2012**, *20*, 628−640.

(28) Noel, J. K.; Whitford, P. C.; Onuchic, J. N. The Shadow Map: A General Contact Definition for Capturing the Dynamics of Biomolecular Folding and Function. *J. Phys. Chem. B* **2012**, *116*, 8692−8702.

(29) Van Der Spoel, D.; Lindahl, E.; Hess, B.; Groenhof, G.; Mark, A. E.; Berendsen, H. J. C. GROMACS: Fast, Flexible, and Free. *J. Comput. Chem.* **2005**, *26*, 1701−1718.

(30) Lammert, H.; Schug, A.; Onuchic, J. N. Robustness and Generalization of Structure-Based Models for Protein Folding and Function. *Proteins: Struct., Funct., Bioinf.* **2009**, *77*, 881−891.

(31) Lua, R. C.; Wilson, S. J.; Konecki, D. M.; Wilkins, A. D.; Venner, E.; Morgan, D. H.; Lichtarge, O. UET: a Database of Evolutionarily-Predicted Functional Determinants of Protein Sequences That Cluster as Functional Sites in Protein Structures. *Nucleic Acids Res.* **2016**, *44*, D308−D312.

(32) Shang, Z.; Zhou, K.; Xu, C.; Csencsits, R.; Cochran, J. C.; Sindelar, C. V. High-Resolution Structures of Kinesin on Microtubules Provide a Basis for Nucleotide-Gated Force-Generation. *eLife* **2014**, *3*, e04686.

(33) Fisher, M. E.; Kolomeisky, A. B. Simple Mechanochemistry Describes the Dynamics of Kinesin Molecules. *Proc. Natl. Acad. Sci. U.S.A.* **2001**, *98*, 7748−7753.

(34) Kolomeisky, A. B.; Fisher, M. E. Molecular Motors: a Theorist's Perspective. *Annu. Rev. Phys. Chem.* **2007**, *58*, 675−695.

(35) Fisher, M. E.; Kolomeisky, A. B. The Force Exerted by a Molecular Motor. *Proc. Natl. Acad. Sci. U.S.A.* **1999**, *96*, 6597−6602.

(36) Cross, R. A. The Kinetic Mechanism of Kinesin. *Trends Biochem. Sci.* **2004**, *29*, 301−309.

DOI: 10.1021/acs.jpcb.8b00830
J. Phys. Chem. B 2018, 122, 4653−4661

(37) Moyer, M. L.; Gilbert, S. P.; Johnson, K. A. Pathway of ATP Hydrolysis by Monomeric and Dimeric Kinesin. *Biochemistry* **1998**, *37*, 800−813.

DOI: 10.1021/acs.jpcb.8b00830
J. Phys. Chem. B 2018, 122, 4653−4661